

Electronic supplementary information

***In operando* XAS investigation of reduction and oxidation processes in cobalt and iron mixed spinels during the chemical loop reforming of ethanol**

F. Carraro,^{a, †} O. Vozniuk,^{b, †} L. Calvillo,^a L. Nodari,^c C. La Fontaine,^d F. Cavani,^b S. Agnoli*^a

^a Department of Chemical Sciences, University of Padova, via Marzolo 1, Padua 35131, Italy

^b Dipartimento di Chimica Industriale “Toso Montanari”, Università di Bologna, Bologna, Italy

^c Istituto di Chimica della Materia Condensata e di Tecnologie per l'Energia. CNR- ICMATE and INSTM, Padova, Italy

^d Synchrotron SOLEIL, Saint Aubin, France

Experimental details

Characterization

XAS data were analyzed using the software based on the IFEFFIT library, ATHENA and ARTEMIS.¹ The XANES spectra were separated into different chemical species using the Linear Combination Fitting (LCF) analysis. Normalized spectra of the corresponding metallic Fe, Co, FeO, CoO, Fe₃O₄, Co₃O₄, Fe₂O₃, fresh ferrite and cobaltite were used as predictor components. EXAFS fits were performed employing two clusters of atoms, one having the absorbing atom in tetrahedral site (A site, considering the general formula of a normal spinel AB₂O₄) and one having the absorbing atom in octahedral site (B site, considering the general formula of a normal spinel AB₂O₄).² Within this model, the parameter $x_b(M)$ is the fraction of A (Fe in FeCo₂O₄ or Co in CoFe₂O₄) cations in octahedral sites. Consequently, the occupation of tetrahedral sites by B cations, which also corresponds to the inversion parameter γ , is defined by the parameter $x_a(M)=1-x_b(M)$. It has to be noticed that the fraction of M³⁺ in B sites must satisfy the requirement $x_b(Fe^{3+})=(2-x_b(Co^{2+}))/2$ in the case of CoFe₂O₄ and $x_b(Co^{3+})=(2-x_b(Fe^{3+}))/2$ in the case of FeCo₂O₄. In the two clusters used for simulating EXAFS spectra, the coordination numbers N_i were kept fixed, whereas R_i (interatomic distance of the i^{th} shell), $2\sigma_i^2$ (mean square displacement about the half-path length of the i^{th} path) and E_0 (energy shift) were free to vary.

The specific surface area was measured applying the single-point BET method, using a Carlo Erba Sorptly 1700.

Energy Dispersive X-ray Spectroscopy of the as prepared materials were acquired using a field emission electron source equipped with a GEMINI column (Zeiss Supra VP35), and confirmed the expected chemical composition of the two fresh catalysts.

Mössbauer spectroscopy was performed on a conventional constant acceleration spectrometer, with a room-temperature (hereafter RT) Rh matrix ⁵⁷Co source, nominal strength 1850 MBq. The hyperfine parameters isomer shift (δ), quadrupole shift (ϵ), full linewidth at half maximum (Γ), were expressed in mms⁻¹ while internal magnetic field (B) in Tesla and the relative area (A) in %. The parameters were obtained by means of standard least-squares minimization techniques. In order to allow the ordering of all the magnetic components and to obtain a good estimation of the sites population, 80 K measurements were performed by using liquid nitrogen static cryostat. 80 K spectra were fitted using the following procedure. Firstly, the spectra were fitted with the minimum number of sextet, whose parameters are indicative of the octahedral and tetrahedral population.³ Once estimated the degree of inversion, defined as the Fe(III) population in the tetrahedral sites, γ the spinel stoichiometry was determined.

Then the fitting procedure was improved considering the effect of tetrahedral next-nearest (NN) neighbour on the octahedral sites, as suggested in literature.² Assuming a statistical occupation of tetrahedral sites by Fe(III) and Co, the magnetic pattern of the octahedral sites was fitted with the proper number of sextet obtained by applying a binomial distribution:

$$P(m) = \frac{6!}{m!(6-m)!} \gamma^m (1-\gamma)^{6-m}$$

$P(m)$ represents the probability of finding m Fe atoms in a shell of NN neighbor tetrahedral sites, depending on the degree of inversion, γ . The obtained results were used to determinate the numbers of sub-components of the octahedral sites and their relative area.

Reactivity experiments were carried out by loading 400 mg of the pelletized sample (with particles diameter ≈ 0.25 to 0.6 mm) in the fixed-bed quartz flow reactor with an internal diameter of 12 mm and a length of 30 cm. The products were monitored on-line by an Agilent 3000A micro-GC with 3 parallel columns: (A) a PlotQ column, with He carrier, for the separation of CH₄, CO₂, H₂O, ethylene, ethane, propane, etc.; (B) a OV1 column, with He carrier, for the separation of ethanol, CO₂, acetaldehyde, H₂O, acetone, acetic acid, ethyl acetate, diethyl ether, 2-pentanone, toluene, etc.; (C) a Molecular Sieve 5A column, Ar carrier, for the separation of H₂, O₂, N₂, CH₄, and CO. A Plot U back flash column was installed in order to avoid CO₂ and H₂O poisoning in the third column. Anaerobic oxidation tests were carried out at 450°C (for 20 min) by feeding continuously a stream of ethanol vapors (app. 15 mol%) in N₂; the latter was also used as a standard. Yields of each product were calculated by the same method as described in reference 4.

Sample	γ (EXAFS)	γ (Mössbauer 80K)	SSA, m ² /g (N ₂ adsorption)	Crystallite size, nm (XRD)	Particle size, nm (N ₂ adsorption)
CoFe ₂ O ₄	0,8	0,74	69	12	16,2
FeCo ₂ O ₄	0,6	0,56	4	32	275

Table S1:
Summary of materials properties: degree of inversion

Temperature of reduction	Sample name	C %	H %
T-350°C	FeCo ₂ O ₄	0.31	0.11
	CoFe ₂ O ₄	1.53	0.42
T-450°C	FeCo ₂ O ₄	5.64	0.15
	CoFe ₂ O ₄	10.65	0.18

surface area, crystallite size and particle size.

Table S2: *C,H,N,S analysis of reduced samples (20 min in ethanol atmosphere: 15 mol % of ethanol in N₂)*

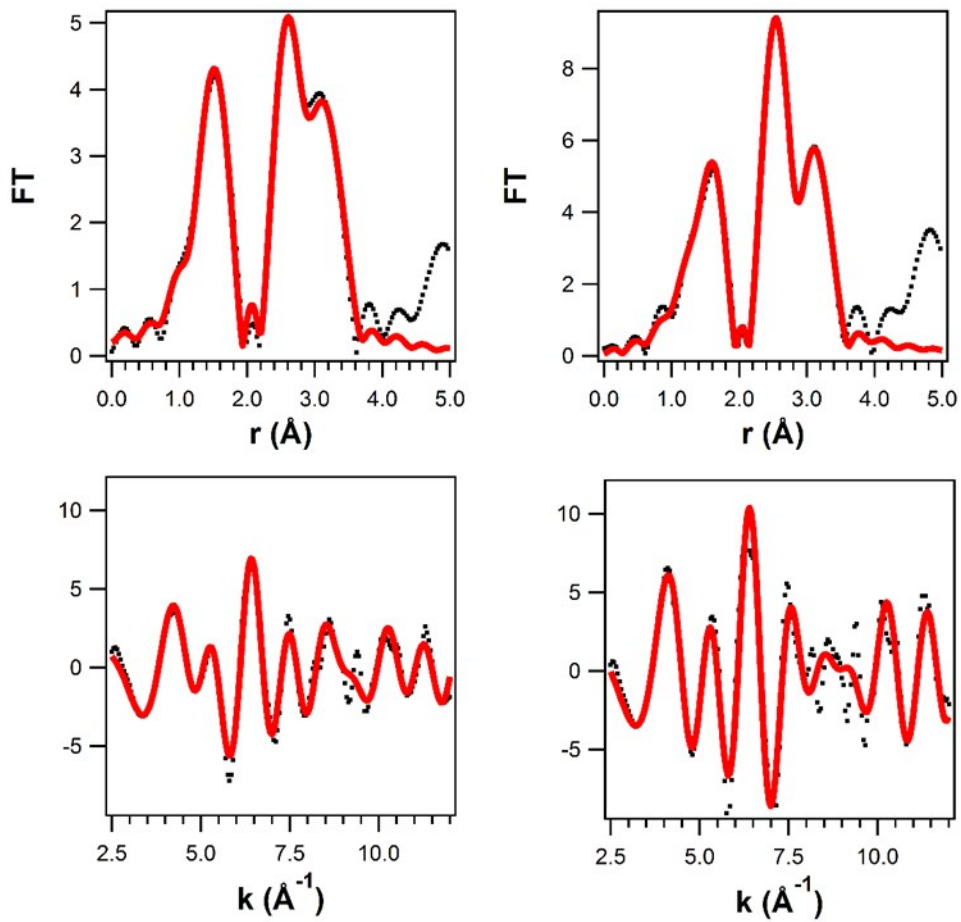


Figure S1: k^3 weighted (bottom) experimental data (black) and fit (red) with the corresponding Fourier transform (top) for the CoFe_2O_4 spinel recorded at the Fe K (left) and Co K (right) edges

Table S3: fit parameters of CoFe_2O_4 , R -factor=0.007

Fe K edge ($E_0= 1.27$)				Co K edge ($E_0= 1.31$)			
Shell	N	R/Å	$\sigma^2 / \text{Å}^2$	Shell	N	R/Å	$\sigma^2 / \text{Å}^2$
$x_B = 0.58$				$x_B = 0.83$			
Fe _{Oh} -O ₁	6	2.02 ± 0.01	0.005 ± 0.002	Co _{Oh} -O ₁	6	2.01 ± 0.02	0.007 ± 0.002
Fe _{Oh} -M _{Oh}	6	2.90 ± 0.01	0.007 ± 0.002	Co _{Oh} -M _{Oh}	6	2.94 ± 0.02	0.008 ± 0.002
Fe _{Oh} -M _{Th}	6	3.49 ± 0.01	0.006 ± 0.002	Co _{Oh} -M _{Th}	6	3.445 ± 0.02	0.008 ± 0.002
$x_A = 0.42$				$x_A = 0.17$			
Fe _{Th} -O ₁	4	1.952 ± 0.009	0.006 ± 0.002	Co _{Th} -O ₁	4	1.98 ± 0.03	0.01 ± 0.004
Fe _{Th} -M _{Oh}	12	3.445 ± 0.009	0.009 ± 0.004	Co _{Th} -M _{Oh}	12	3.48 ± 0.02	0.006 ± 0.002
Fe _{Th} -M _{Th}	4	3.478 ± 0.009	0.030 ± 0.009	Co _{Th} -M _{Th}	4	3.51 ± 0.03	0.008 ± 0.003
				Co _{Th} -O ₂	4	3.63 ± 0.03	0.006 ± 0.003

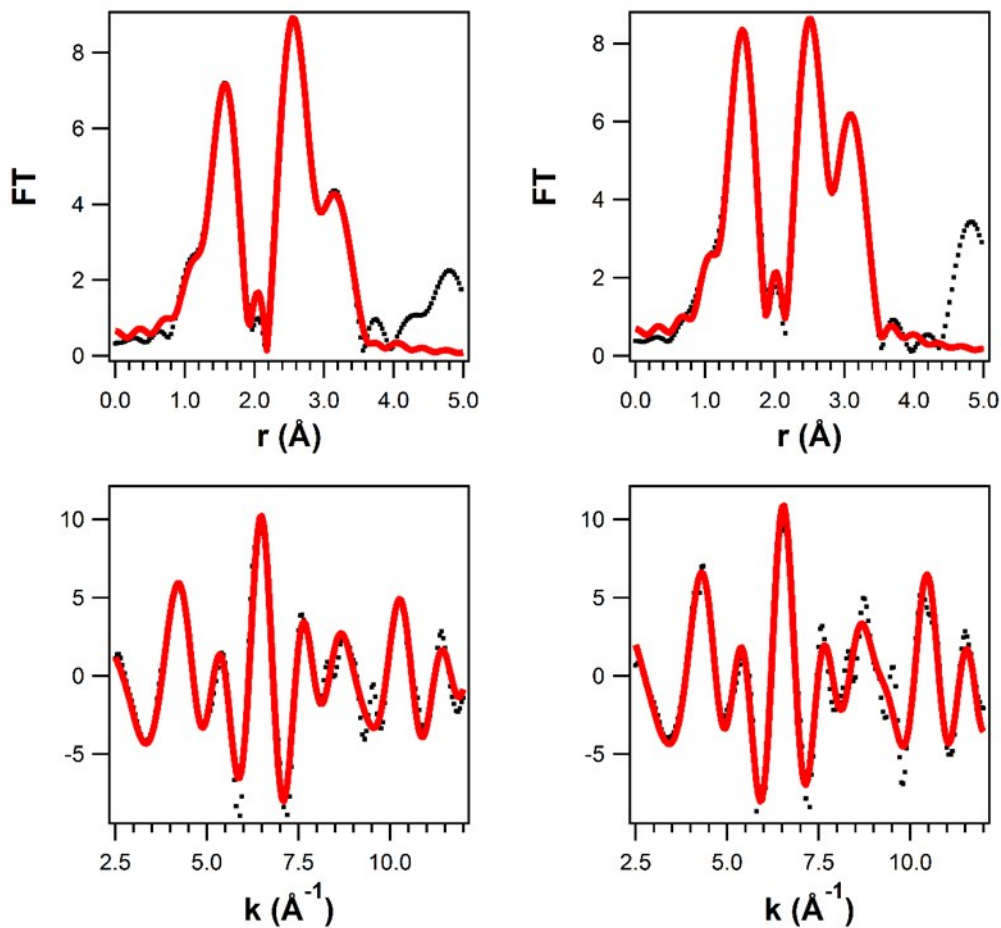


Figure S2: k^3 weighted (bottom) experimental data (black) and fit (red) with the corresponding Fourier transform (top) for the FeCo_2O_4 spinel recorded at the Fe K (left) and Co K (right) edges

Table S4: fit parameters of FeCo_2O_4 , R -factor=0.007

Fe K edge ($E_0=2.86$)				Co K edge ($E_0=4.24$)			
Shell	N	R/Å	$\sigma^2 / \text{Å}^2$	Shell	N	R/Å	$\sigma^2 / \text{Å}^2$
$x_B = 0.64$				$x_B = 0.68$			
$\text{Fe}_{\text{Oh}}\text{-O}_1$	6	$1,993 \pm 0.006$	0.008 ± 0.002	$\text{Co}_{\text{Oh}}\text{-O}_1$	6	1.97 ± 0.02	0.009 ± 0.007
$\text{Fe}_{\text{Oh}}\text{-M}_{\text{Oh}}$	6	2.951 ± 0.006	0.006 ± 0.001	$\text{Co}_{\text{Oh}}\text{-M}_{\text{Oh}}$	6	2.91 ± 0.02	0.006 ± 0.002
$\text{Fe}_{\text{Oh}}\text{-M}_{\text{Th}}$	6	3.474 ± 0.006	0.008 ± 0.003	$\text{Co}_{\text{Oh}}\text{-M}_{\text{Th}}$	6	3.43 ± 0.02	0.005 ± 0.004
$x_A = 0.36$				$x_A = 0.32$			
$\text{Fe}_{\text{Th}}\text{-O}_1$	4	1.98 ± 0.03	0.002 ± 0.001	$\text{Co}_{\text{Th}}\text{-O}_1$	4	1.93 ± 0.03	0.006 ± 0.003
$\text{Fe}_{\text{Th}}\text{-M}_{\text{Oh}}$	12	3.49 ± 0.01	0.008 ± 0.003	$\text{Co}_{\text{Th}}\text{-M}_{\text{Oh}}$	12	3.52 ± 0.01	0.011 ± 0.006
$\text{Fe}_{\text{Th}}\text{-O}_2$	4	3.49 ± 0.01	0.009 ± 0.003	$\text{Co}_{\text{Th}}\text{-M}_{\text{th}}$	4	3.70 ± 0.02	0.009 ± 0.003

Table S5: 80 K Mössbauer parameters for iron cobaltite and cobalt ferrite. P(1), P(2), P(3), P(4) represent the different NN neighbour configurations. δ is quoted to α -Fe, using a 6-lines calibration.

FeCo_2O_4	δ (mm/s)	ε (mm/s)	Γ (mm/s)	B (T)	A (%)
Tetrahedral Site	0.33	-0.02	0.42	49.7	44
Octahedral Site, P(4)	0.41	0.003	0.26	53.2	11
Octahedral Site, P(3)	0.49	0.01	0.32	50.5	18
Octahedral Site, P(2)	0.39	-0.02	0.27	50.8	18
Octahedral Site, P(1)	0.42	0.019	0.40	46.2	9
CoFe_2O_4					
Tetrahedral Site	0.29	-0.03	0.74	48.8	37
Octahedral Site, P(4)	0.47	0.02	0.26	53.0	9
Octahedral Site, P(3)	0.37	-0.03	0.33	52.7	17
Octahedral Site, P(2)	0.41	-0.05	0.29	51.02	22
Octahedral Site, P(1)	0.44	0.03	0.30	52.25	15

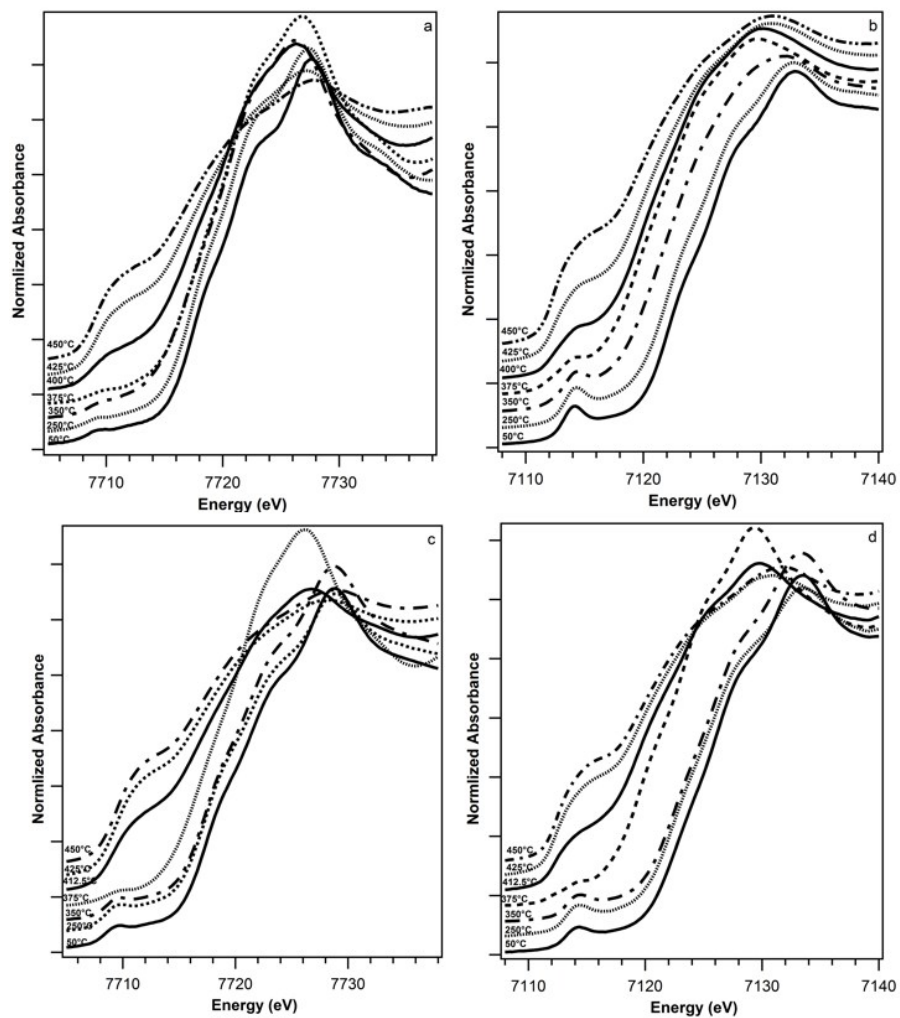


Figure S3: XANES spectra at Co (a,c) and Fe(b,d) K-edge for CoFe_2O_4 (a,b) and FeCo_2O_4 (c,d) during the annealing treatment in reducing atmosphere (0.69 % ethanol in N_2)

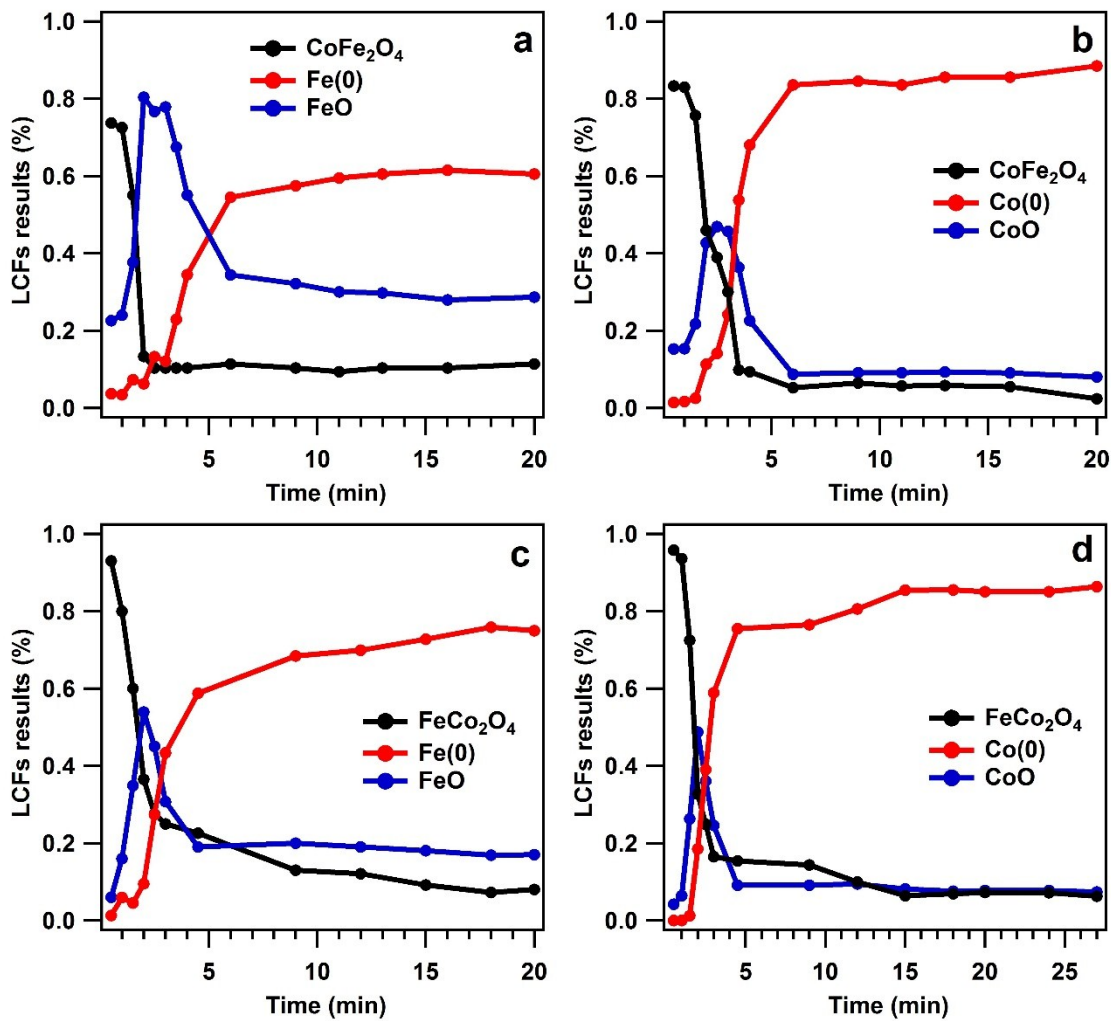


Figure S4: LCFs (% of composition vs temperature) of Fe(b,c) and Co (a,c) K-edge for FeCo₂O₄ (a,b) and CoFe₂O₄ (c,d) during the treatment in reducing atmosphere (5.3 % ethanol in N₂) at 450°C.

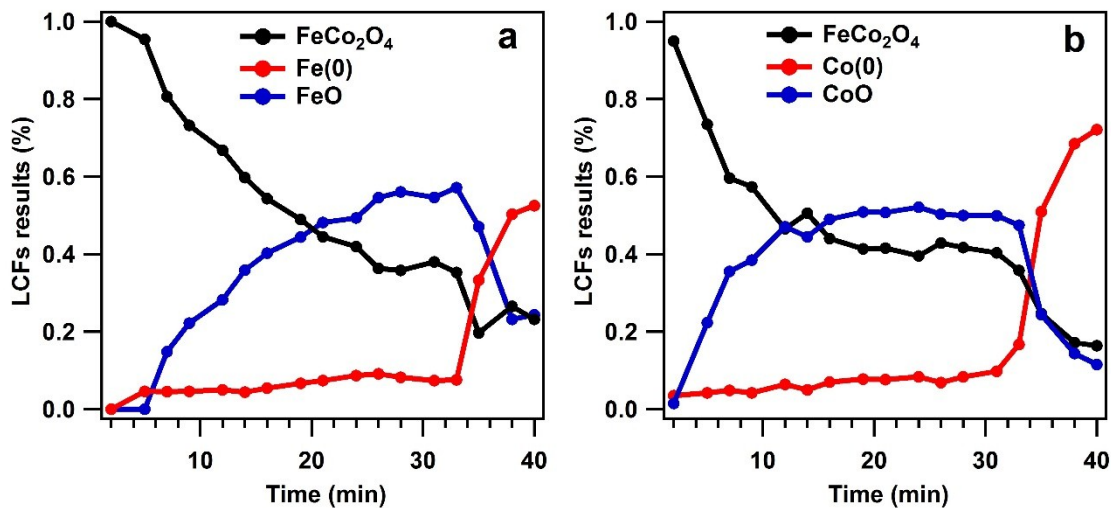


Figure S5: LCFs (% of composition vs temperature) of Fe(b) and Co (a) K-edge for FeCo_2O_4 (a,b) during the treatment in reducing atmosphere (0.69 % ethanol in N_2) at 450°C .

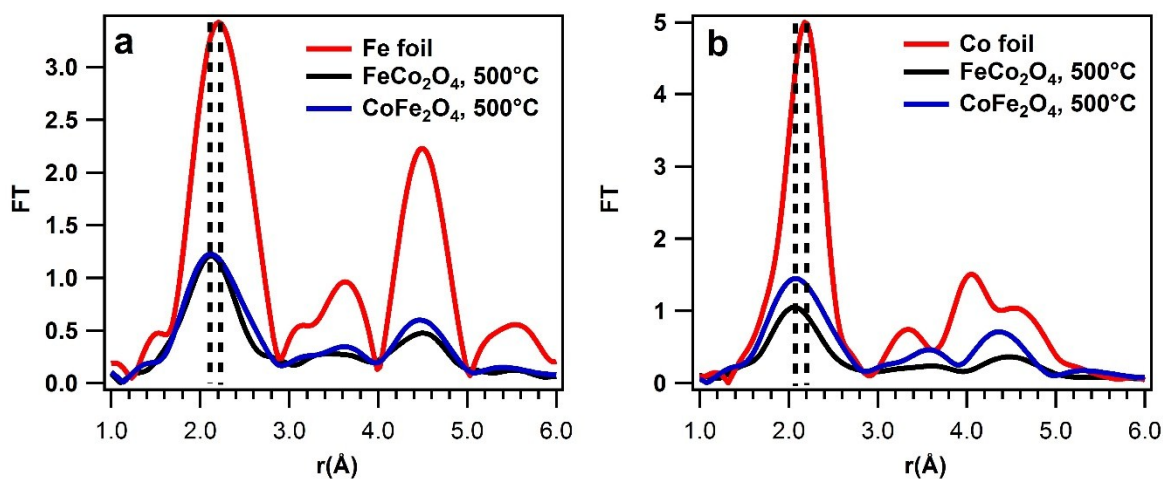


Figure S6: Fourier transform EXAFS of the CoFe_2O_4 and of FeCo_2O_4 at the end of the annealing in ethanol atmosphere (500°C) recorded at the Fe K (a) and Co K (b) edges. The FT EXAFS spectra of the reduced samples are compared with the FT EXAFS of Fe and Co metal foils.

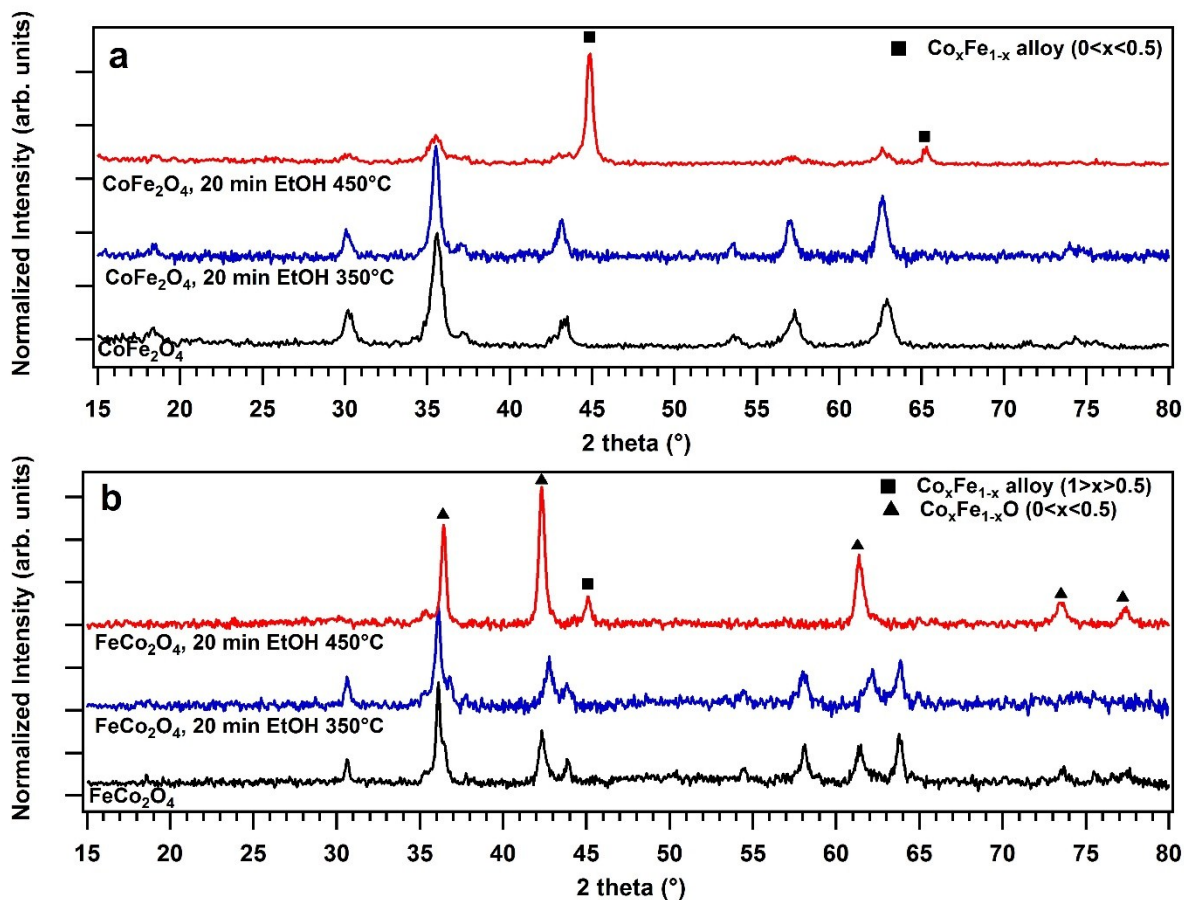


Figure S7: XRD patterns of a) CoFe_2O_4 and b) FeCo_2O_4 of as prepared samples and after 20 minutes at 350°C and 450°C in reductive atmosphere (15 mol % of ethanol in N_2)

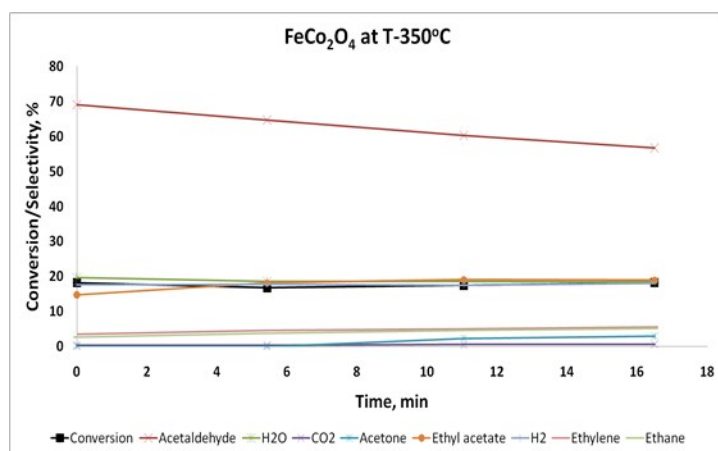


Figure S8 : Conversion and Selectivities to the main products obtained for FeCo_2O_4 during 20 min reduction at $T=350^\circ\text{C}$

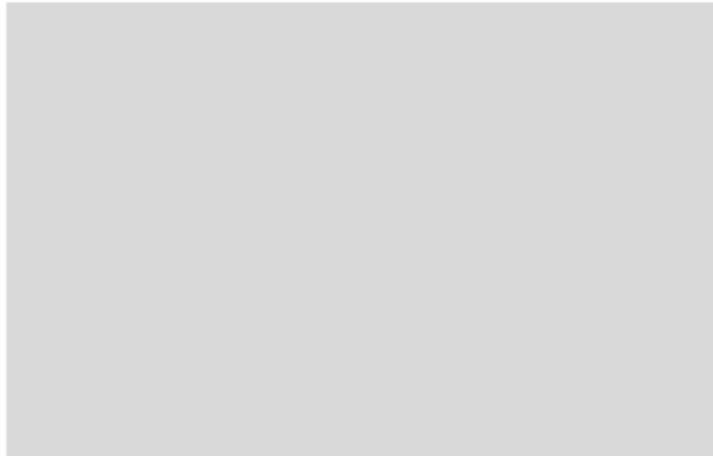


Figure S9: Conversion and Selectivities to the main products obtained for CoFe_2O_4 during 20 min reduction at $T=350^\circ\text{C}$

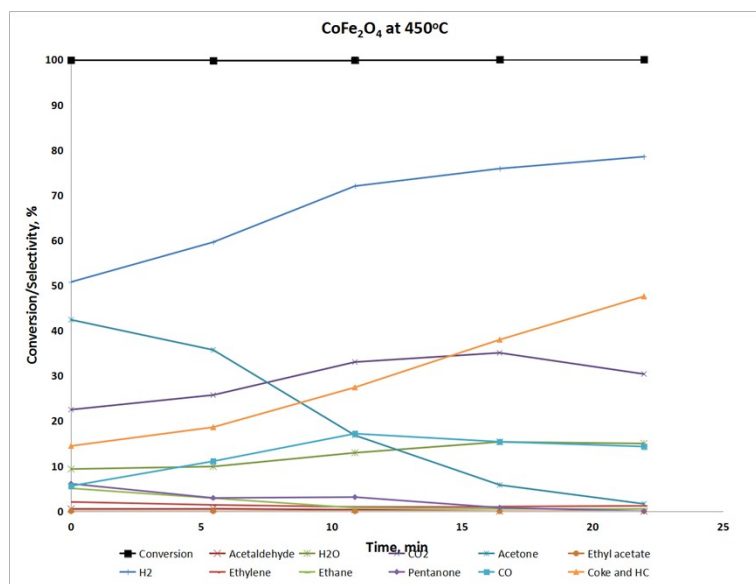


Figure S10: Conversion and Selectivities to the main products obtained for CoFe_2O_4 during 20 min reduction at $T=450^\circ\text{C}$

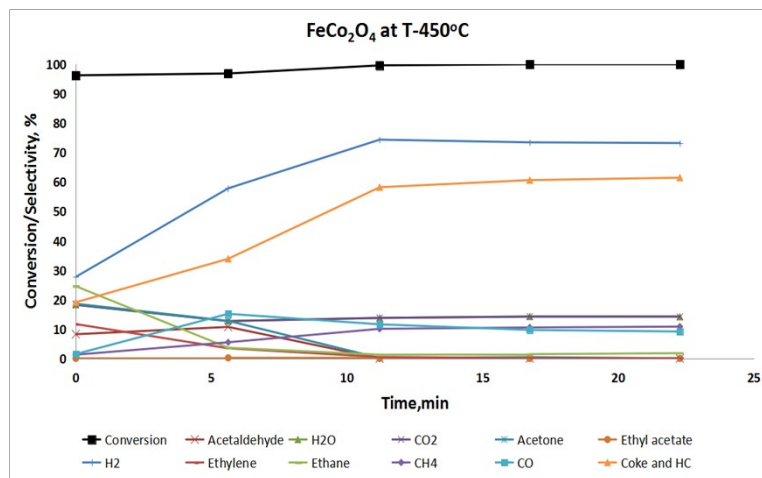


Figure S11: Conversion and Selectivities to the main products obtained for FeCo₂O₄ during the 20 min reduction at T-450°C

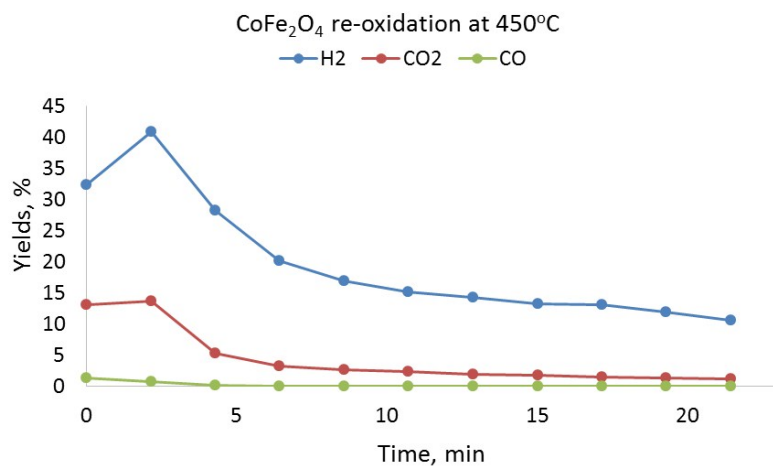


Figure S12 : Yields to H₂ and CO_x obtained over CoFe₂O₄ during 20 min of re-oxidation with water at 450°C

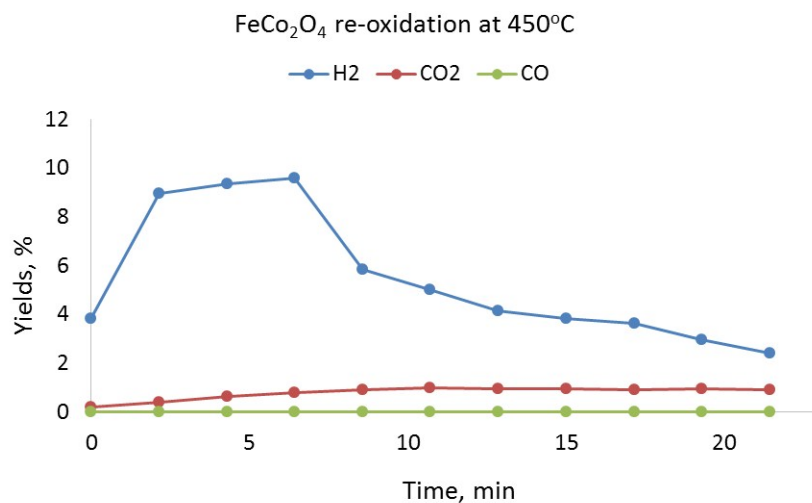


Figure S13 : Yields to H₂ and CO_x obtained over FeCo₂O₄ during 20 min of re-oxidation with water at 450°C

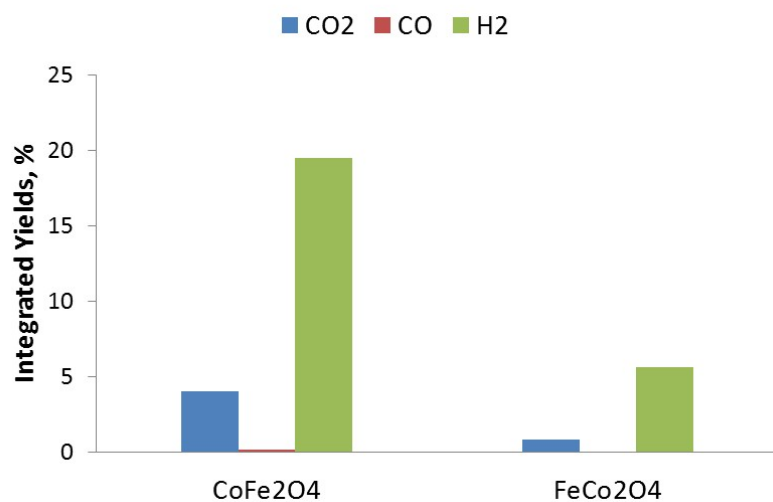


Figure S14 : Integrated yields to H₂, CO_x obtained over CoFe₂O₄ and FeCo₂O₄ during 20 min re-oxidation with water at 450°C

References

- ¹ B.Ravel; M. Newville, *Synchrotron Radiat.*, 2005, **12**, 537–541.
- ² D.Carta; M. F.Casula; A.Falqui; D.Loche; G.Mountjoy; C.Sangregorio; A.Corrias, *J. Phys. Chem. C*, 2009, **113** (20), 8606–8615.
- ³ C.N.Chinnasamy; A.Narayanasamy; N.Ponpandian; K.Chattopadhyay; K.Shinoda; B.Jeyadevan; K.Tohji; K.Nakatsuka; T.Furubayashi; I.Nakatani, *Phys. Rev. B*, 2001, **63**, 184108.
- ⁴ C.Trevisanut; O.Vozniuk; M.Mari; S.Yurena; A.Urrea; C.Lorentz; J.-M.Millet; F. Cavani, *Top. Catal.*, 2016, **59**, 1600–1613